THE UNIVERSITY MICHIGAN

COLLEGE OF ENGINEERING
Department of Electrical Engineering
Space Physics Research Laboratory

ORA Project 07301

PITOT MEASUREMENTS ON SPARROW ARCAS VEHICLES

by

Jack J. Horvath

Contract No. AF 19(628)-5069
Project No. 6682
Task No. 668202
Work Unit No. 66820201

FINAL REPORT

Period Covered: 1 April 1965 through 31 August 1968

June 1969

Contract Monitor: Gerard A. Faucher
Aerospace Instrumentation Laboratory

Prepared
for

AIR FORCE CAMBRIDGE RESEARCH LABORATORIES
OFFICE OF AEROSPACE RESEARCH
UNITED STATES AIR FORCE
BEDFORD, MASSACHUSETTS 01730

administered through:

OFFICE OF RESEARCH ADMINISTRATION ANN ARBOR, MICHIGAN 48105

ABSTRACT

Radioactive ionization gages were used as sensors for pitot measurements on two Sparrow-Arcas boosted payloads launched on 7 and 8 February 1969. Pressure, temperature, and density were obtained in the region 38 to 70 km. Both graphical and tabulated data are presented.

Both the vehicle system performance and the payload performance were excellent. Modification of the ionization gage sensitivity would permit data acquisition to 105 km.

TABLE OF CONTENTS

LIST OF TABLES

LIST OF FIGURES

1. INTRODUCTION

The research activity described in this report is a direct result of the continuing need to extend meteorology to higher altitudes. Basic instrumentations used by present day meteorologists to explore structure in the upper atmosphere consist of balloon and rocket borne sondes. The rocket borne sondes, instrumented with temperature sensitive thermistors, are limited, technically, to altitudes below 60 km. Approximately 1500 Arcas class vehicles are launched each year from fourteen (14) major locations in the western hemisphere. Continued efforts by many groups to extend the thermistor technique to higher altitudes have been unsuccessful.

A program (Atlantic Research Corporation, 1965) was initiated in 1963 to develop a low cost meteorological rocket probe system to measure pressure/density to an altitude in excess of 100 km. The pitot probe technique used with this system was an adaptation of pitot probe instrumentations used in other programs (Horvath, Simmons, and Brace, 1962; Horvath and Rupert, 1968). Fourteen tests of the rocket payloads were performed with varying degrees of success.

The purpose of the present research effort in the Sparrow Arcas (Sparc) program was to extend the initial Atlantic Research developmental program by increasing the accuracy and reliability of the Atlantic Research Corporation (ARC) payload. Two Sparc payloads were successfully launched in February 1968. Both payloads performed to the limit of their design capability. The density profiles obtained are not indicative of the ultimate capability of the Sparc type system. The ionization gages used in the Sparc program were volume-limited with the consequent loss of low pressure (high altitude) sensitivity. Ionization gage designs are available with sensitivities capable of carrying the Sparc probe measurement to approximately 105 km. These gage design characteristics are included in the report.

2. INSTRUMENTATION

The payload used in the Sparc program is similar in concept to that used in the original ARC research effort. In fact, the payloads, void of sensor and sensor electronics, were supplied by ARC as government furnished equipment. The major difference between the Denpro and Sparc payloads is the sensor. The Denpro used a diaphragm type pressure sensor with questionable reliability. The Sparc payload is instrumented with a radioactive ionization gage similar to that used in other pitot probe applications. In addition the Arcasonde III instrument section (part of the ARC payload) was modified in such a way that it would not be a limiting factor in outputting sensor data.

The Sparc payload is shown in Figure 1.

A. EJECTABLE TIP

The ejectable tip is an ogive nose cone fabricated from a phenolic material (Figure 1). It performs the dual function of providing the necessary low drag frontal configuration for the Sparrow-Arcas vehicle during the boost phase and of sealing the pitot measurement chamber against undesirable contamination prior to its ejection after the second stage burnout (approximately 40 km in altitude).

The spring-loaded nose cone is held in place by three steel pins located symmetrically in a plane normal to the cone axis. Release of the nose cone is effected by a pyrotechnic gas generator which displaces three sealed pistons, thus forcing the three steel retaining pins free of the payload. The concentrically loaded spring then ejects the nose cone and the separation assembly forward from the payload at an initial relative forward velocity of approximately 20 ft/sec. Upon ejection the nose cone acts as an unstable body and will pitch-yaw away from the vehicle flight path, thus exposing the pitot orifice to a previously undisturbed atmosphere.

A first motion mechanical time provides the timing logic in the ejection process, and the pyrotechnic generator is actuated by a charged capacitor.

B. PITOT SENSOR

The impact pressure sensing device used with the Sparc system consists of a radioactive-type ionization gage. Ionization gage devices are actually sensitive to gas density but are normally calibrated in terms of pressure. For data correction purposes, the gas temperature (gage wall temperature) must be carefully noted. The current-pressure characteristic for the gages used in

this program are shown in Figure 2.

The linear current-pressure (density) characteristic represents, in effect, the collection of positive ions resulting from alpha particle bombardment and ionization of the neutral gas in the gage volume. The emission element is an Americium 241 source which emits alpha particles. Appropriate internal gage geometry and electric field potentials provide the desired current-pressure relation.

Radioactive ionization gage sensors have an ultimate upper altitude limitation for a pitot measurement on an ascending rocket probe of approximately 110 km. The altitude capability of the two Sparc payloads was on the order of 70 km. This limitation was the result of a restriction placed upon the physical size of the ionization gage by the geometry of the Sparc payload and does not represent a limitation of the system for future application at the higher altitudes. Redesign of the Sparc payload, permitting the use of a more sensitive ionization gage, would extend the measuring capability of the Sparc payload to approximately 105 km. Figure 3 shows the characteristic current-pressure relation for a radioactive ionization gage capable of this increased performance.

C. SIGNAL PREPARATION

A linear multirange electrometer amplifier is used to match the impedance of the low output current ionization gage to the rocket borne telemetry package. An integral amplifier sensitivity selection circuit maintains a voltage output from the amplifier between 0 and 5 volts to be compatible with telemetry requirements. The amplifier signal is outputted through a five (5) channel multiplexer which periodically inserts two (2) channel voltage calibrations along with gage temperature and amplifier range data. The 1680 MHz cavity oscillator transmitter is modulated with the multiplexed output through a Vector Model MMO-11 subcarrier oscillator (S.C.O.). A complete functional block diagram is shown in Figure 4.

D. MAGNETIC ASPECT SENSOR

An important requisite on a rocket payload system instrumented for a pitot measurement is vehicle stability. To isolate the gross aspects of vehicle attitude, a polarized magnetic aspect sensor was included in each of the two Sparc payloads. The output from the magnetic sensor can be interpreted in terms of the angle between the magnetic field vector, B, and the vehicle thrust axis. For a stable flight the vehicle thrust axis would, within a few degrees, be tangent to the velocity vector. Since the velocity vector changes very slowly in both direction and magnitude, fluctuations in the magnetic sensor output will immediately indicate irregular flight characteristics. It is not necessary to have an accurately calibrated device to determine if and when an irregular event took place.

The main purpose for using the magnetic sensor was to evaluate vehicle stability during and after nose cone ejection. The initial Sparc flights gave no indicated perturbation in vehicle attitude as a function of nose cone ejection. Changes in angle of 2-3 degrees would have been detectable.

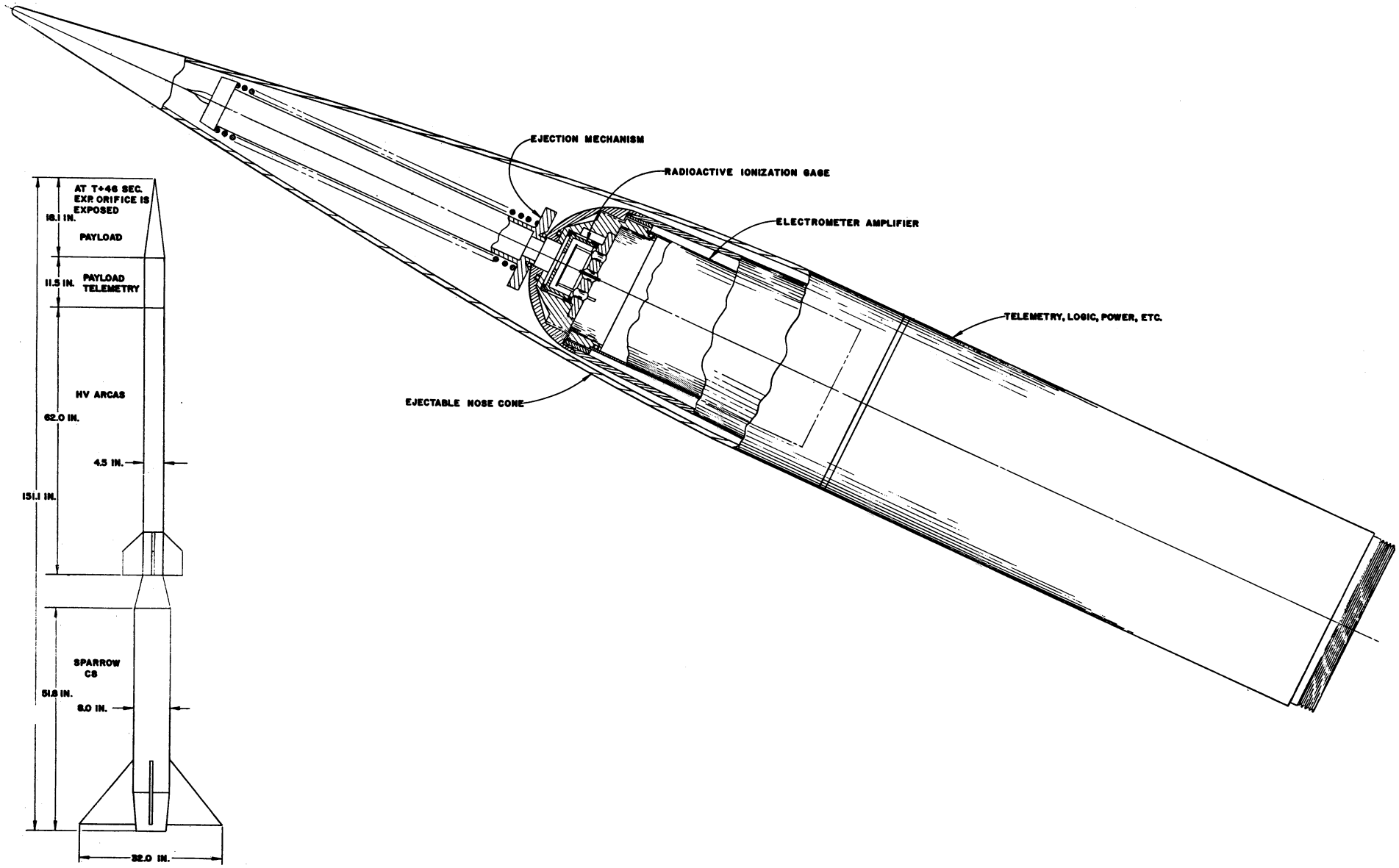

Figure 1. Sparc payload.

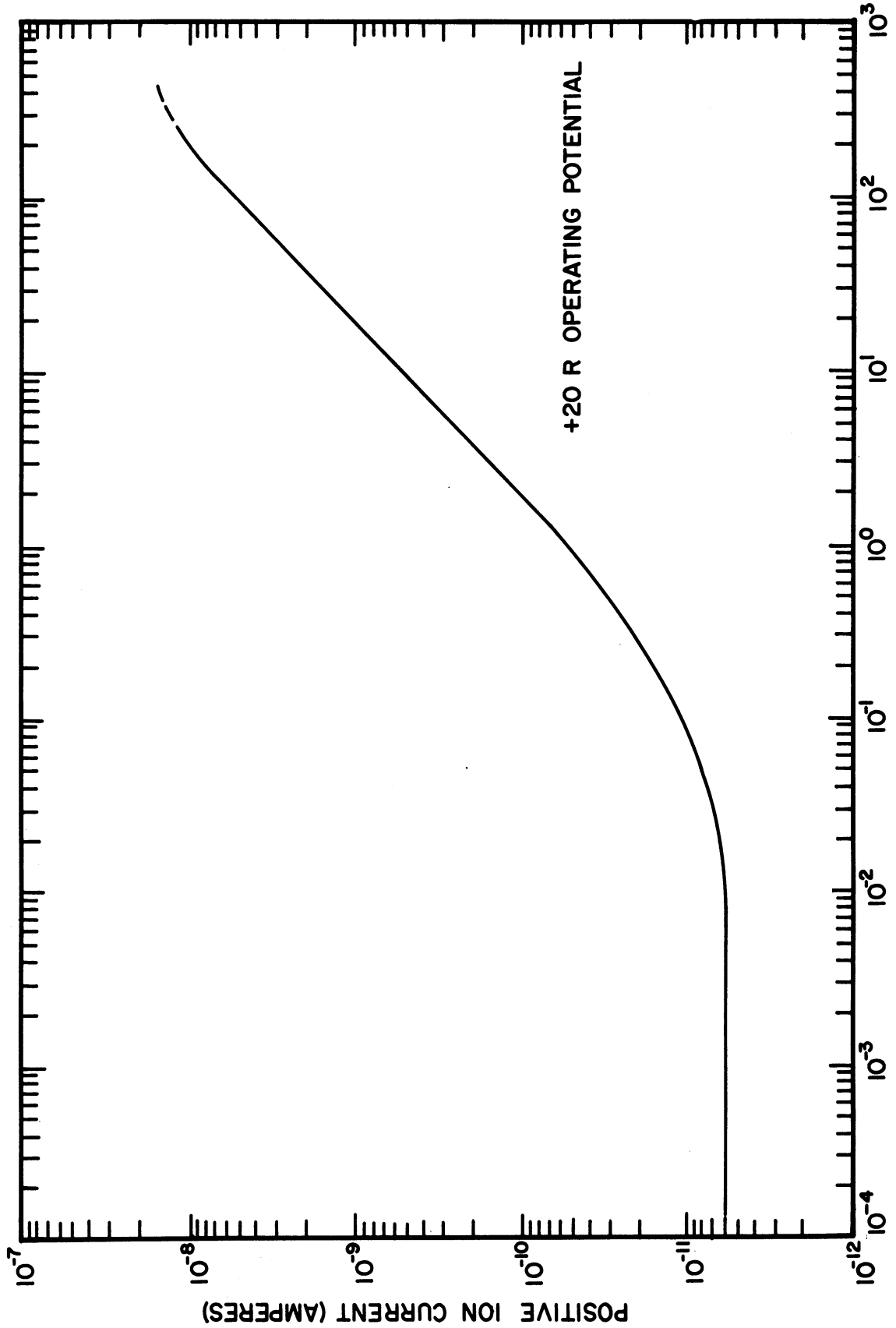

Figure 2. Sparc ionization gage characteristic.

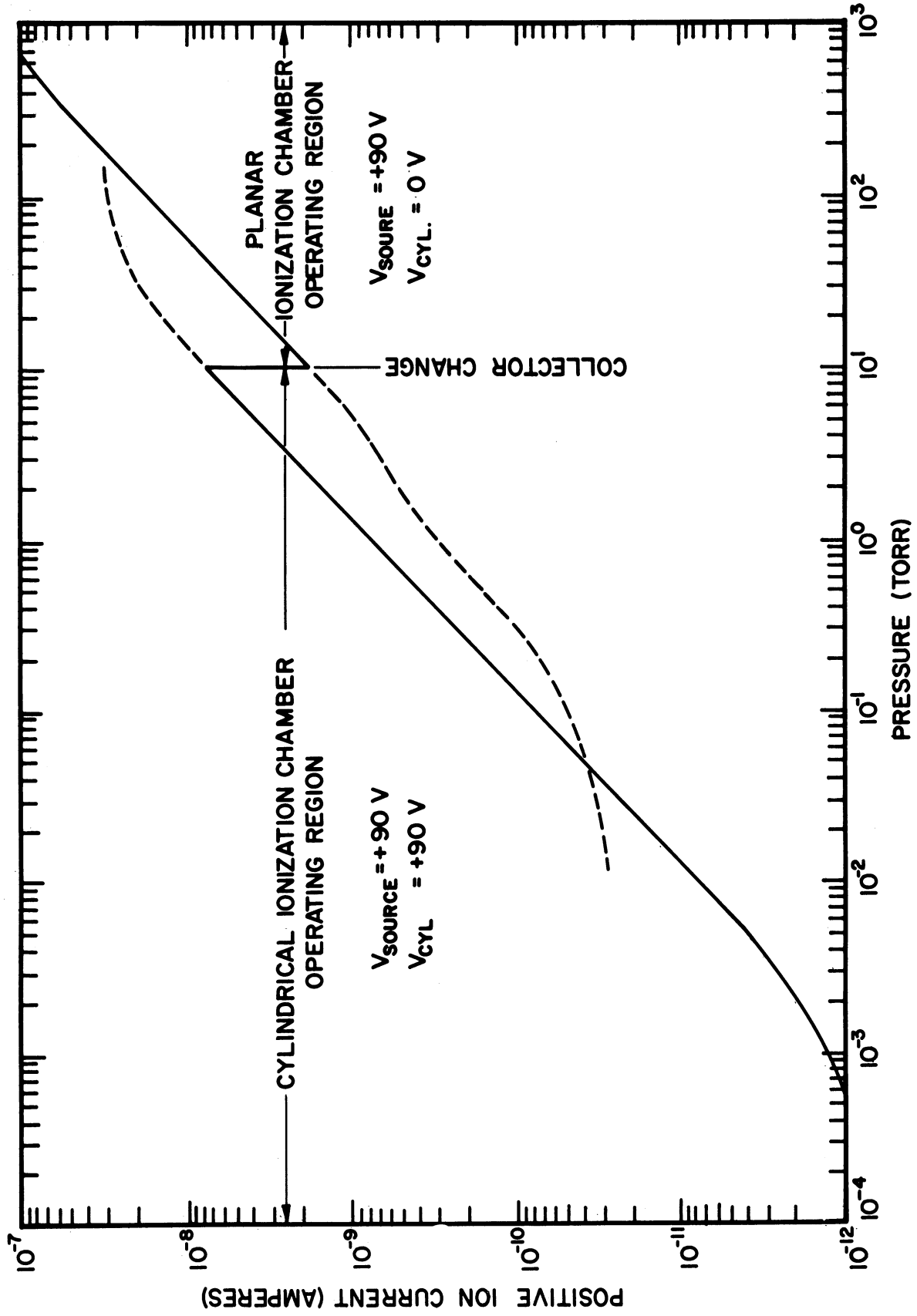

Figure 3. Dual collector ionization gage characteristic.

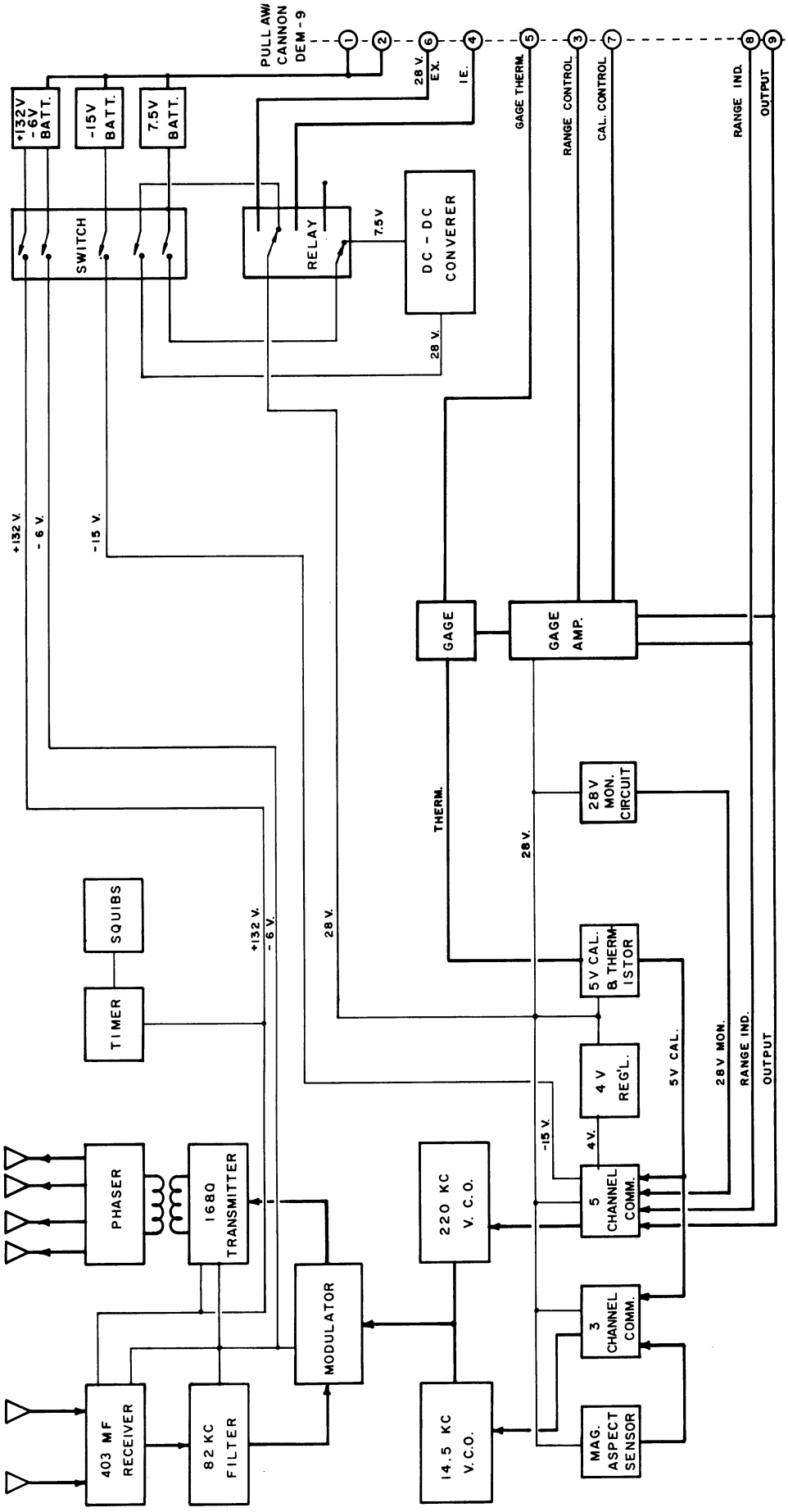

Figure 4. Sparc functional block diagram.

3. PROCEDURES

The basic atmospheric structure parameter derived from a pitot measurement is ambient density. The equation used in the density reduction,

$$\rho_a = \frac{1435\ Pi}{K(M,\gamma)\ V^2}\ (Kg/m^3),$$

is one form of the Rayleigh supersonic pitot tube equation using the relationship

$$\frac{Pi}{Pa} = F(M,\gamma) \qquad \text{(Shapiro, 1953)}$$

where

Pi = impact pressure,
Pa = ambient pressure,
ρ_a = ambient density,
M_a = Mach number (V/a),
γ = ratio of specific heats, 1.4,
$K(M,\gamma)$ = weak function of both M and γ,
V = rocket total velocity,
a = velocity of sound.

The Rayleigh expression is applicable in the continuum flow regime (below 85 km). For the two Sparrow Arcas pitot payloads discussed in this report, continuum conditions hold throughout the measurement region. The function, $K(M,\gamma)$, is a weak function of both Mach number and specific heats. During the measurement region it varies less than 3% over the Mach range observed.

A. ANGLE OF ATTACK

A basic assumption in the pitot measurement theory requires that a normal shock front exist at the impact pressure orifice. This requires that the angle of attack be relatively small. Angle of attack sensitivity is unique to individual nose cone configurations. Wind tunnel testing (Laurmann, 1958) shows that the hemispherical nose tip similar to the Sparc payload design has an angle of attack error of 1% at 12°. The output data from the magnetic aspect sensor indicate very little deviation between vehicle thrust axis and the velocity vector during the time pitot measurements are being made. Errors due to angle of attack are estimated to be less than 0.2%.

B. ATMOSPHERIC WIND EFFECTS

Strong horizontal winds, in the plane of the flight path, can cause sizeable errors in the resultant density profiles by their effect on the total velocity vector. The Rayleigh density expression

$$\rho_a = \frac{1435\ Pi}{K(M,\gamma)|Ve|^2}$$

requires an appropriate value of Ve. In the presence of a horizontal atmospheric wind, the effective velocity component, Ve, is equal to

$$|Ve| = |V| \pm |W_H| \text{ Sin } \Sigma \text{ Cos } \psi$$

where

V = total inertial velocity,
$|W_H|$ = magnitude of horizontal wind,
Σ = 90 - Q.E.
Q.E. = quadrant elevation,
ψ = angle between the flight path plane and wind direction.

The quantity, $|W_H|$ Sin Σ Cos ψ, can be maintained negligibly small compared to V if Σ is a reasonably small angle and/or ψ is very nearly 90°. The magnitude of the Σ angle during the measurement period (37-70 km) is a function of the initial effective Q.E. and, to a lesser degree, the altitude of vehicle at apogee. The effective launch elevation angle (Q.E.) for both Sparc payloads was less than 80°. In the altitude increment from 37 to 70 km, Σ angles ranged from 20° to 23.5°. The flight path azimuth was 234°. The atmospheric wind structure was a typical Pt. Mugu winter profile, predominately zonal winds from the west and increasing monotonically from 30 m/sec at 37 km to 80 m/sec at 50 km. Meridional winds were negligibly small. The angle, ψ, is simply the difference angle between the flight path azimuth and the wind direction or 36°. The magnitude of Ve for the two Sparc flights is

$$|Ve| = |V| \pm |W_H| \text{ Sin } \Sigma \text{ Cos } 36°$$

with $20 < \Sigma < 23.5°$.

The W_H profiles are shown in Figure 5. Density error profiles resulting from atmospheric winds are shown in Figure 6.

The angle of attack error caused by these same horizontal winds has been neglected, being at least one order of magnitude less than wind effect on the velocity vector magnitude.

It should be noted that errors due to atmospheric winds can be reduced significantly by proper consideration of the angles Σ and Ψ.

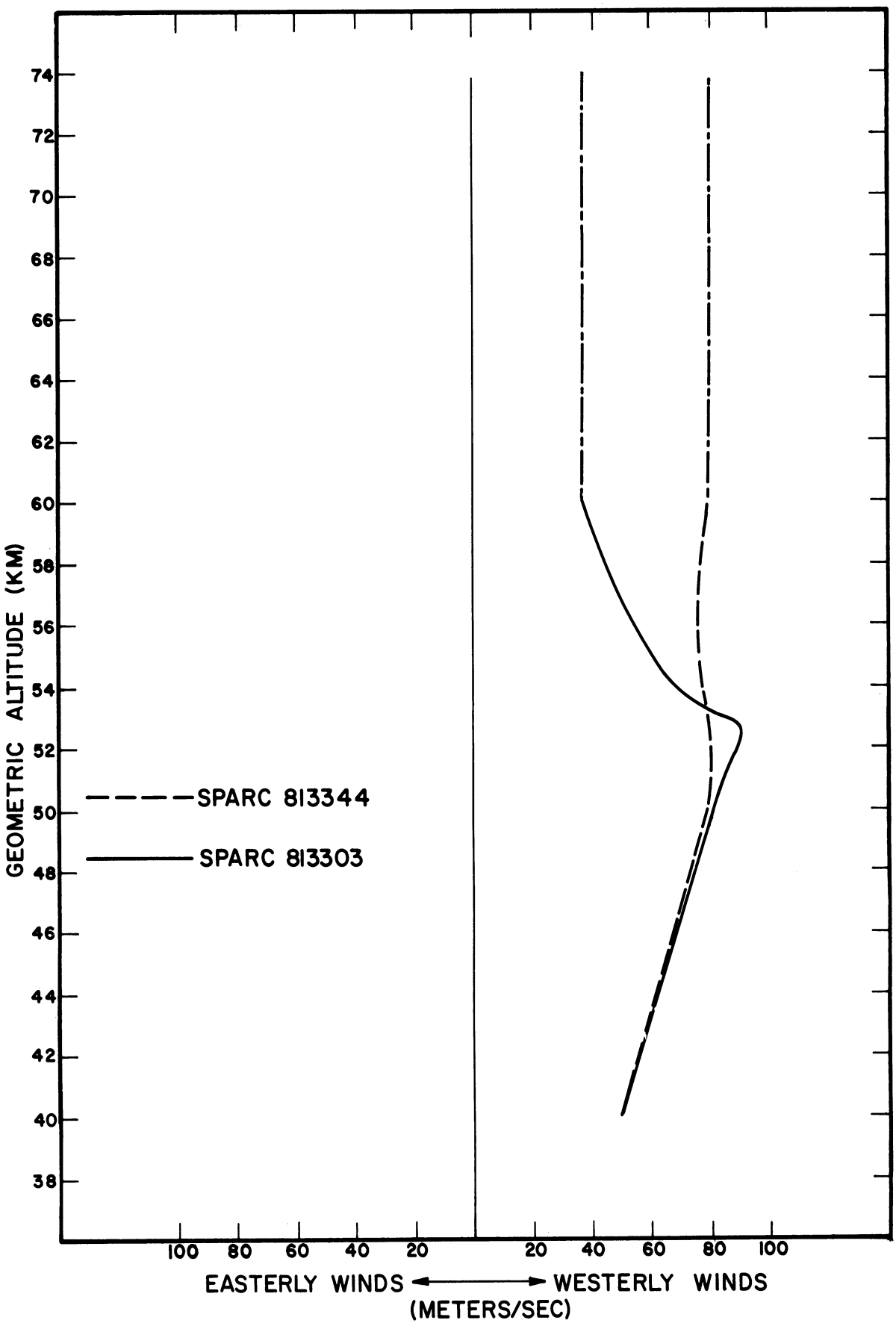

Figure 5. Zonal horizontal wind profiles.

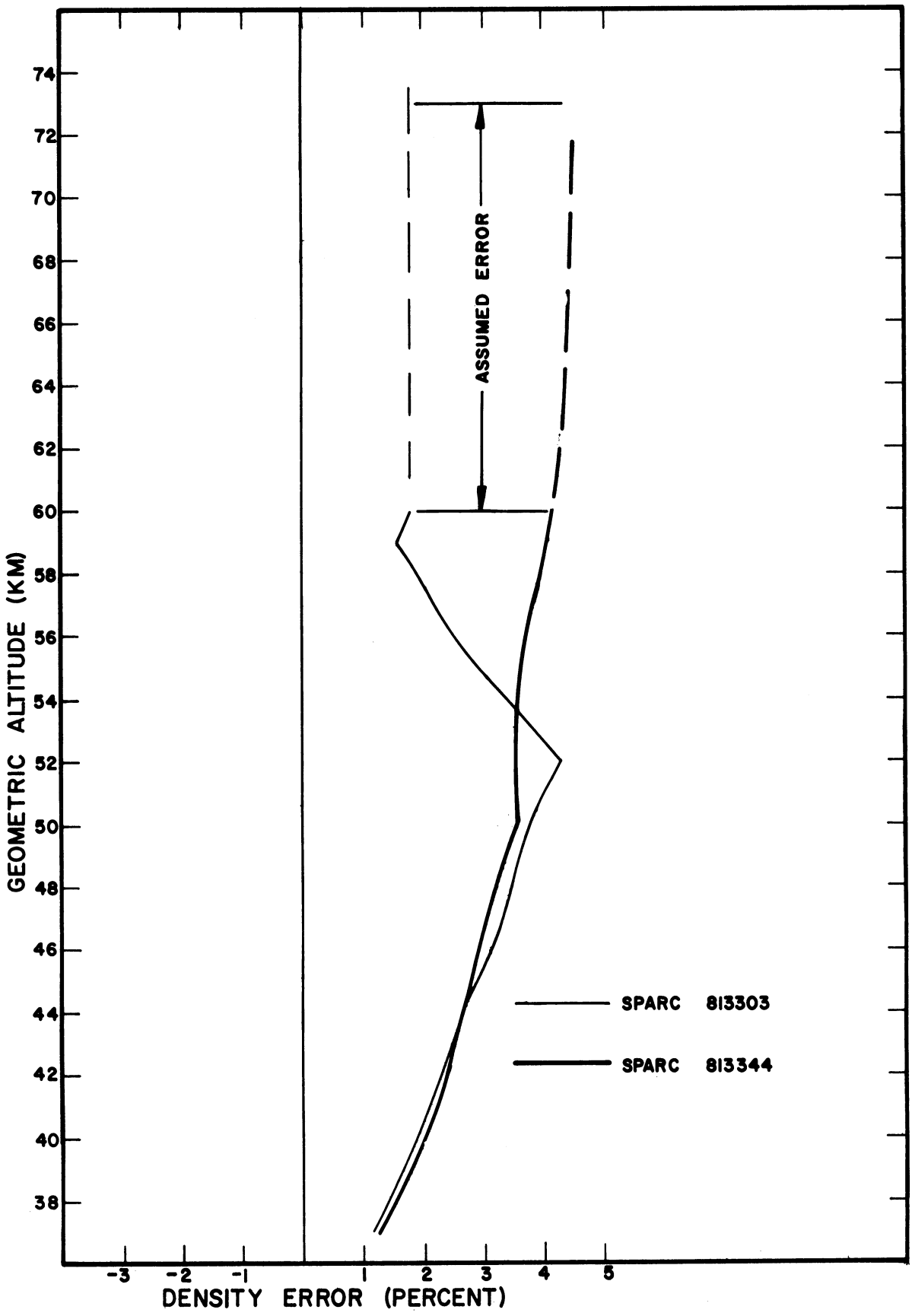

Figure 6. Density errors due to horizontal winds.

4. DATA

The telemetered data were recorded on magnetic tape at the Pt. Mugu Mobile G.M.D. 2 Ground Station. The basic G.M.D. 2 system was modified so as to permit FM discrimination of the two output data channels. Both real time and playback paper records were obtained. Reduction of the data to atmospheric structure information was accomplished entirely by manual processes. The data could easily be reduced by computer techniques if large quantities of data were to be handled.

Tracking data for trajectory determination were obtained from the FPS-16 radar facility at Pt. Mugu. Tabulated reduced trajectory data were furnished by Pt. Mugu.

A. STATISTICAL DATA

General flight information relating to the two Sparc launches are given in Tables 1 and 2. The launch of both payloads proceeded without difficulty. Each Sparc launch was associated with a corresponding Arcasonde 1A experiment. For comparison, these data are graphed with the pitot data.

B. ATMOSPHERIC STRUCTURE

Ambient atmospheric density profiles are the direct result of impact pressure measurements on a pitot probe. The density profiles shown in Figures 9 and 12 have been corrected for errors due to horizontal atmospheric winds. The estimated accuracy of the density data are ± 2% below 60 km and ± 4% above 60 km. The assumed wind structure above 60 km accounts for the increased density error flags.

Ambient temperature (Figures 8 and 11) and pressure (Figures 7 and 10) are derived from the density profile by integration of the hydrostatic equation. Integration takes place:

$$dP = -\rho g dH, \quad P = -\int_{h_o}^{h} \rho g dH + P_o$$

$$h_o > h$$

$$\text{or} \qquad T = \frac{\rho_o}{\rho} T_o - \frac{1}{\rho R} \int_{h_o}^{h} \rho g dH$$

from higher to lower altitudes. The boundary condition was assumed equal to the temperature from the U.S. Standard Atmosphere, 1962 at the starting altitude

of integration. The rate at which temperature and/or pressure converge to their ideal values during integration depends upon the scale height. For the scale heights found in this region, convergence of the data will be better than 1% of the absolute value after integrating over 15 km. Integration intervals were selected to be 0.5 km.

The estimated accuracy of the temperature data are

$$\begin{aligned} &3^\circ \text{ K} < 55 \text{ km}, \\ 55 \text{ km} < &5^\circ \text{ K} < 60 \text{ km}, \\ 60 \text{ km} < &7^\circ \text{ K} < 65 \text{ km}, \\ 65 \text{ km} < &10^\circ \text{ K} \end{aligned}$$

for the indicated altitude increments. The large error flags above 55 km are the direct result of the unknown starting temperature value used in the integration process.

Accuracy of the pressure profiles, like the temperature data, increases as the downward integration continues. Estimated accuracy of the pressure data are

$$\begin{aligned} &2\% < 55 \text{ km}, \\ 55 \text{ km} < &3\% < 60 \text{ km}, \\ 60 \text{ km} < &5\% < 65 \text{ km}, \\ 65 \text{ km} < &6\% \end{aligned}$$

for the indicated altitude increments.

The ambient atmospheric data derived from Sparc 813303 and Sparc 813344 are tabulated in Tables 3 and 4.

TABLE 1

STATISTICAL DATA - Sparc 813303

Sparc Pitot Probe
Table of Flight Parameters

Launch Time: 19:58:03.55 GMT

Launch Date: 07 February 1968

Location: Pt. Mugu Long: 119°07'W
Lat: 34°07'N

Payload Weight: 18.7 lbs

Event	Flight Time (sec)	Altitude (km)
Life-off	0	
1st Stage Burnout	2 (est)	
2nd Stage Ignition	8 (est)	4.5 (est)
2nd Stage Burnout	39.5	29.5
Tip Ejection	45.3	38
Limit of Usable Data	72.5	70
Peak Altitude	182.5	129.2

TABLE 2

STATISTICAL DATA - Sparc 813344

Sparc Pitot Probe
Table of Flight Parameters

Launch Time: 19:34:17.43 GMT

Launch Date: 08 February 1968

Location: Pt. Mugu Long: 119°07'W
Lat: 34°07'N

Payload Weight: 18.7 lbs

Event	Flight Time (sec)	Altitude (km)
Lift-off	0	
1st Stage Burnout	2 (est)	
2nd Stage Ignition	8 (est	4.5 (est)
2nd Stage Burnout	39 (est)	29 (est)
Tip Ejection	45.4	37.5
Limit of Usable Data	74.9	73
Peak Altitude	185.4	130.8

TABLE 3

AMBIENT DATA—SPARC 813303

7 February 1968
11:58 Local
19:58 GMT
Pt. Mugu

Long. 119°07'W
Lat. 34°07'N

Altitude (km)	Density (kg/m^3)	Temperature (°K)	Pressure (torr)	ρ/ρ_{std}	P/P_{std}
37.5	5.76	247.3	3.06×10^{0}	.98	1.01
38.0	5.28×10^{-3}	250.4	2.85	.98	1.01
38.5	4.88	252.5	2.64	.98	1.00
39.0	4.57	252.7	2.48	.99	1.00
39.5	4.30	251.9	2.33	1.00	1.00
40.0	4.02	251.4	2.17	1.01	1.00
40.5	3.74	253.3	2.04	1.01	1.00
41.0	3.46	255.3	1.90	1.00	1.01
41.5	3.21	257.8	1.78	.99	1.01
42.0	2.97	260.4	1.66	.99	1.01
42.5	2.76	262.4	1.56	.99	1.01
43.0	2.57	264.5	1.46	.99	1.01
43.5	2.40	266.6	1.38	.99	1.01
44.0	2.23	268.7	1.29	.99	1.01
44.5	2.11	268.3	1.22	1.00	1.01
45.0	1.98	267.7	1.14	1.01	1.02
45.5	1.86	267.2	1.07×10^{0}	1.01	1.02
46.0	1.74	266.7	9.98×10^{-1}	1.01	1.01
46.5	1.64	266.8	9.40	1.02	1.01
47.0	1.54	266.7	8.83	1.03	1.02
47.5	1.45	266.2	8.31	1.03	1.02
48.0	1.36	265.7	7.78	1.03	1.01
48.5	1.28	265.2	7.30	1.03	1.02
49.0	1.21	264.8	6.89	1.04	1.02
49.5	1.14	263.7	6.47	1.04	1.02
50.0	1.07×10^{-3}	262.6	6.05	1.04	1.01
50.5	9.93×10^{-4}	262.6	5.62	1.04	1.01
51.0	9.42	262.6	5.32	1.04	1.01
51.5	8.83	262.5	4.99	1.04	1.00
52.0	8.28	262.7	4.68	1.04	1.00
52.5	7.83	261.0	4.40	1.04	1.00
53.0	7.37	259.4	4.11	1.04	1.00
53.5	6.91	260.1	3.87	1.03	1.00
54.0	6.43	261.4	3.62	1.02	1.00
54.5	6.02	262.0	3.39	1.02	.99

TABLE 3 (Concluded)

Altitude (km)	Density (kg/m^3)	Temperature (°K)	Pressure (torr)	ρ/ρ_{std}	P/P_{std}
55.0	5.63	262.6	3.18	1.01	.99
55.5	5.30	261.7	2.98	1.00	.99
56.0	4.98	260.7	2.80	1.00	.99
56.5	4.68	259.5	2.61	1.00	.99
57.0	4.42	258.6	2.46	1.00	.99
57.5	4.17	257.5	2.31	1.00	.99
58.0	3.91	256.7	2.16	1.00	.99
58.5	3.71	253.2	2.02	1.00	.99
59.0	3.50	250.9	1.89	1.01	.98
59.5	3.33	246.7	1.77	1.02	.98
60.0	3.15	243.2	1.65	1.03	.98
60.5	2.95	243.2	1.54	1.03	.98
61.0	2.75	243.7	1.44	1.02	.98
61.5	2.58	242.2	1.34	1.02	.98
62.0	2.42	242.1	1.26	1.01	.97
62.5	2.25	242.4	1.17	1.00	.97
63.0	2.11	241.2	1.10	.99	.97
63.5	1.98	239.2	1.02×10^{-1}	.99	.97
64.0	1.85	239.2	9.52×10^{-2}	.98	.97
64.5	1.73	239.7	8.91	.98	.97
65.0	1.61	239.7	8.29	.97	.97
65.5	1.50	239.7	7.73	.96	.97
66.0	1.40	239.1	7.21	.95	.97
66.5	1.31	240.1	6.77	.95	.97
67.0	1.21	242.1	6.30	.93	.98
67.5	1.15	236.3	5.85	.95	.98
68.0	1.09	232.2	5.45	.96	.98
68.5	1.02×10^{-4}	230.5	5.06	.96	.98
69.0	9.78×10^{-5}	223.6	4.70	.98	.98

TABLE 4

AMBIENT DATA—SPARC 813344

8 February 1968
11:34 Local
19:34 GMT
Pt. Mugu

Long. 119°07'W
Lat. 34°07'N

Altitude (km)	Density (kg/m^3)	Temperature (°K)	Pressure (torr)	ρ/ρ_{std}	P/P_{std}
38.0	5.32×10^{-3}	242.9	2.78×10^{0}	.99	.98
38.5	4.94	244.1	2.60	.99	.98
39.0	4.57	246.0	2.42	.99	.98
39.5	4.18	250.3	2.26	.98	.98
40.0	3.86	254.0	2.11	.97	.98
40.5	3.59	256.3	1.98	.96	.98
41.0	3.31	259.6	1.85	.96	.98
41.5	3.09	260.3	1.73	.96	.98
42.0	2.87	262.9	1.62	.96	.98
42.5	2.68	263.7	1.52	.96	.99
43.0	2.51	265.1	1.43	.97	.99
43.5	2.37	264.3	1.35	.98	.99
44.0	2.22	264.0	1.26	.98	.99
44.5	2.09	262.3	1.18	.99	.99
45.0	1.98	260.5	1.11	1.00	.99
45.5	1.86	260.5	1.04×10^{0}	1.00	.99
46.0	1.74	260.5	9.75×10^{-1}	1.01	.99
46.5	1.62	261.3	9.10	1.01	.99
47.0	1.52	262.0	8.56	1.02	.98
47.5	1.41	263.1	7.97	1.02	.98
48.0	1.33	263.7	7.54	1.01	.98
48.5	1.23	267.9	7.08	.99	.98
49.0	1.14	270.8	6.63	.98	.98
49.5	1.08	271.1	6.30	.98	.98
50.0	1.00×10^{-3}	273.0	5.87	.97	.98
50.5	9.52×10^{-4}	270.3	5.53	.98	.98
51.0	8.98	268.7	5.18	.99	.98
51.5	8.45	267.6	4.86	.99	.98
52.0	7.97	267.1	4.57	1.00	.98
52.5	7.53	265.3	4.30	1.00	.98
53.0	7.12	263.7	4.03	1.00	.98
53.5	6.67	262.6	3.77	1.00	.98
54.0	6.32	261.2	3.55	1.00	.98
54.5	5.97	258.8	3.32	1.00	.98

TABLE 4 (Concluded)

Altitude (km)	Density (kg/m^3)	Temperature (°K)	Pressure (torr)	ρ/ρ_{std}	P/P_{std}
55.0	5.65	256.6	3.12	1.01	.97
55.5	5.30	256.3	2.92	1.00	.97
56.0	4.97	256.0	2.74	1.00	.97
56.5	4.71	256.3	2.60	.99	.97
57.0	4.37	256.5	2.41	.99	.97
57.5	4.22	251.3	2.28	1.00	.97
58.0	3.98	246.7	2.11	1.01	.97
58.5	3.77	242.3	1.97	1.01	.96
59.0	3.54	240.2	1.83	1.02	.95
59.5	3.31	239.7	1.70	1.02	.95
60.0	3.09	239.2	1.59	1.01	.94
60.5	2.88	239.6	1.48	1.00	.94
61.0	2.68	240.2	1.38	.99	.93
61.5	2.51	238.5	1.29	.99	.93
62.0	2.35	237.7	1.20	.98	.93
62.5	2.20	235.9	1.12	.97	.93
63.0	2.05	235.1	1.04×10^{-1}	.96	.92
63.5	1.93	234.1	9.74×10^{-2}	.96	.92
64.0	1.80	233.0	9.05	.96	.92
64.5	1.69	231.6	8.42	.95	.91
65.0	1.57	231.2	7.81	.94	.91
65.5	1.48	228.9	7.28	.94	.91
66.0	1.40	224.3	6.76	.95	.91
66.5	1.31	221.7	6.23	.95	.91
67.0	1.23	220.0	5.82	.95	.90
67.5	1.14	219.3	5.38	.95	.90
68.0	1.07×10^{-4}	215.8	4.97	.94	.89
68.5	9.95×10^{-5}	215.0	4.60	.93	.89
69.0	9.25	214.3	4.27	.93	.89
69.5	8.57	213.0	3.97	.92	.89
70.0	7.98	212.0	3.64	.92	.88
70.5	7.38	212.2	3.36	.91	.88
71.0	6.83	211.2	3.10	.90	.87
71.5	6.31	211.4	2.87	.89	.87
72.0	5.82	211.4	2.65	.88	.87
72.5	5.40	210.8	2.45	.88	.87
73.0	5.00×10^{-5}	210.0	2.26	.87	.87

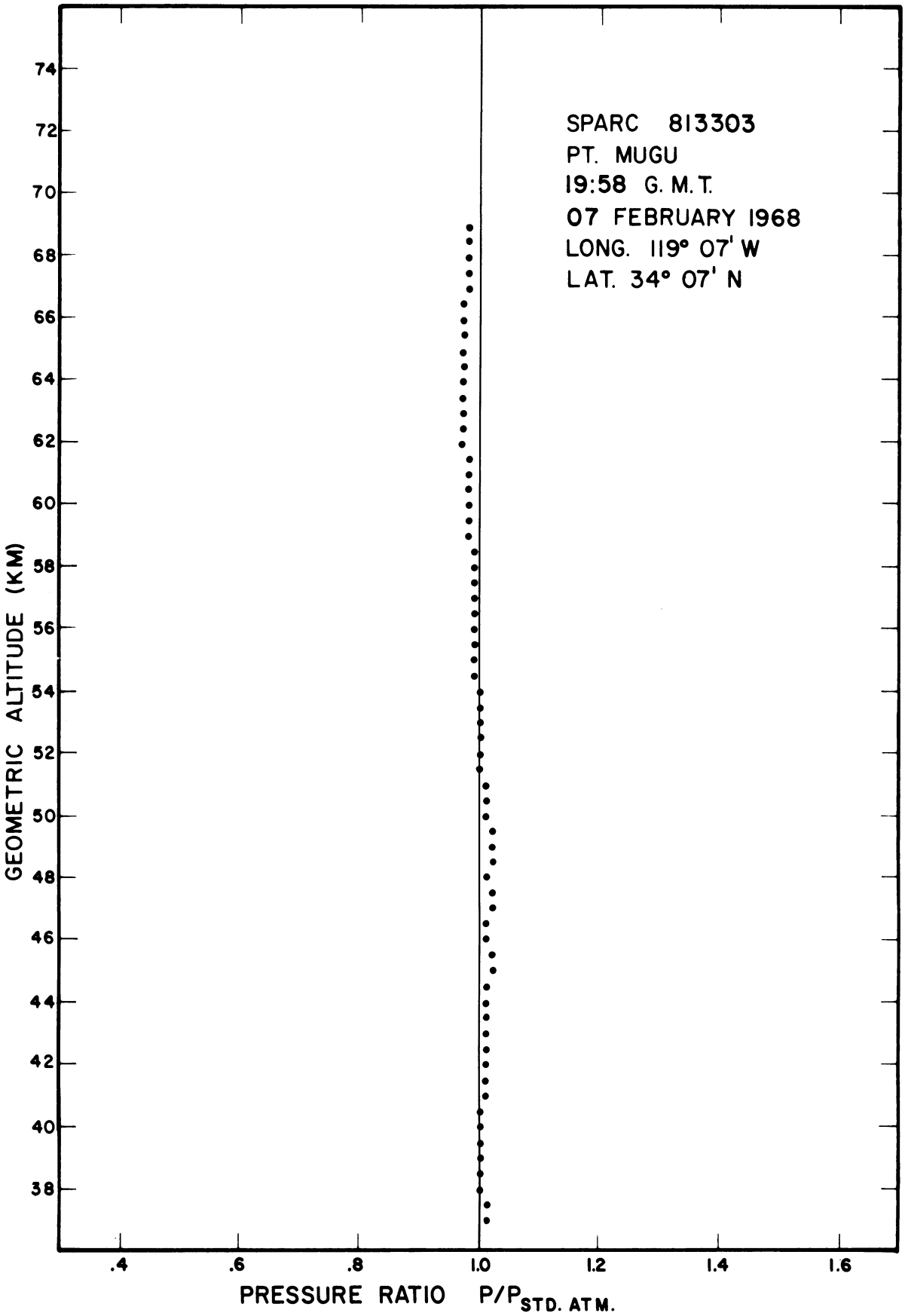

Figure 7. Altitude vs. pressure - Sparc 813303.

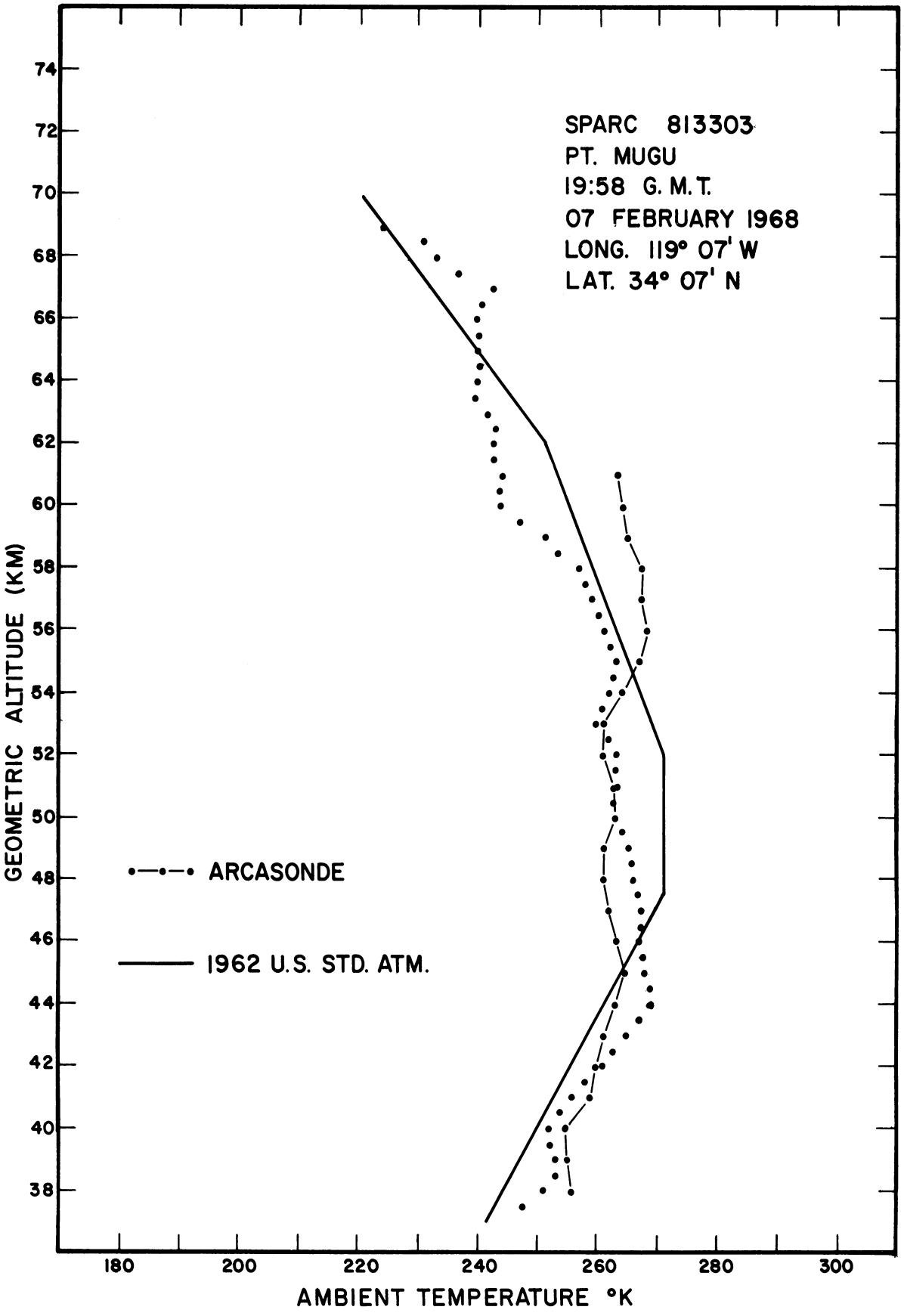

Figure 8. Altitude vs. temperature - Sparc 813303.

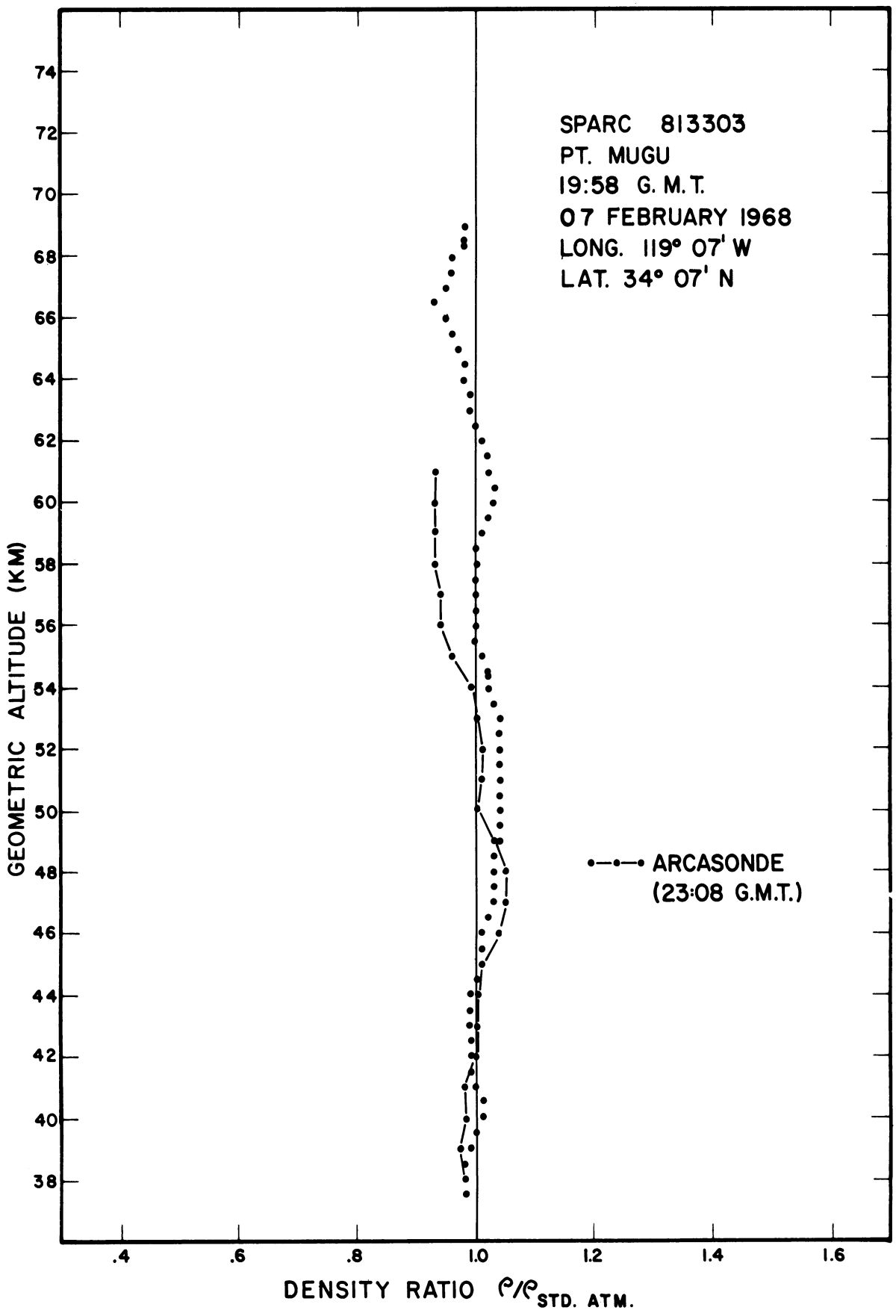

Figure 9. Altitude vs. density - Sparc 813303.

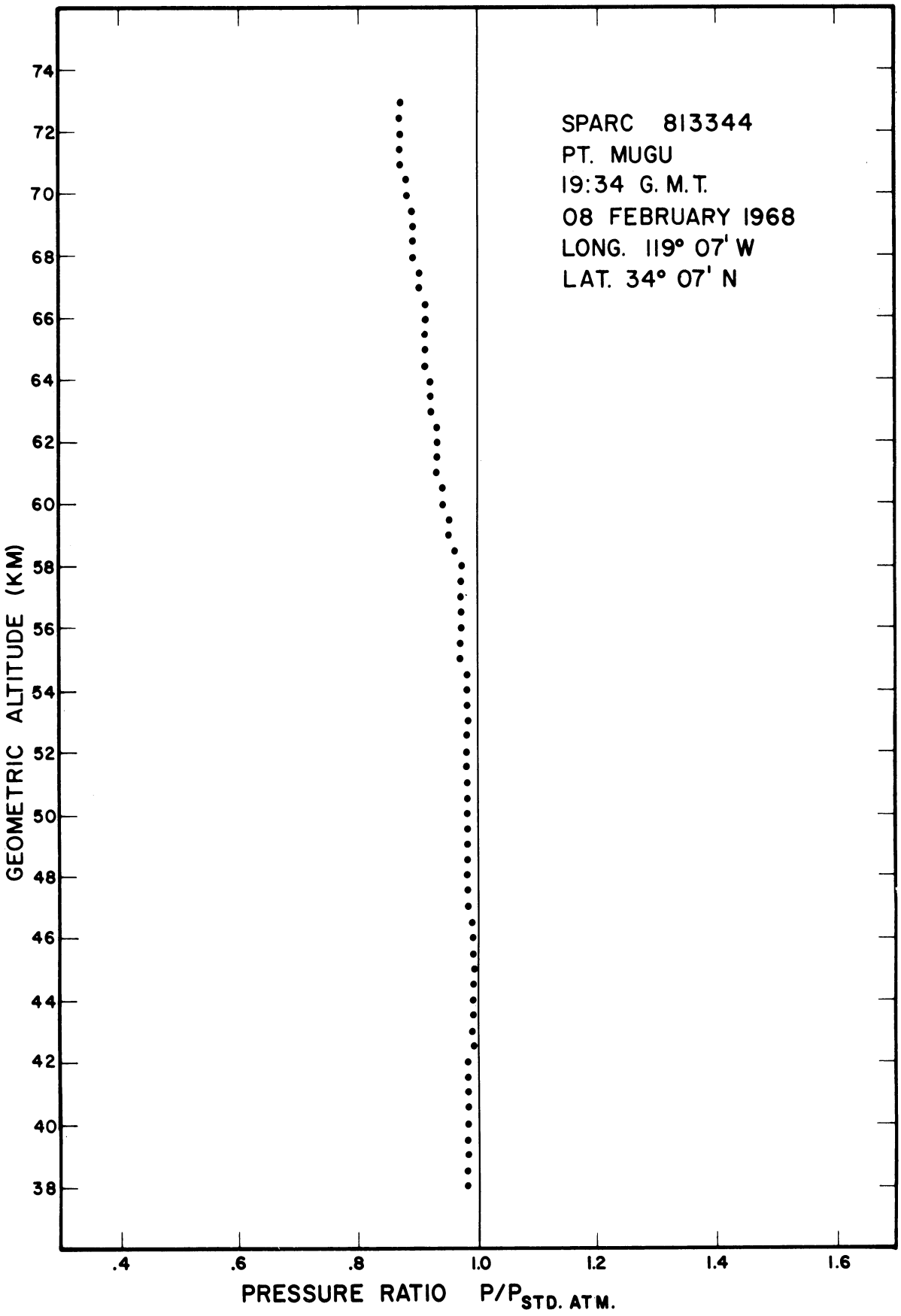

Figure 10. Altitude vs. pressure - Sparc 813344.

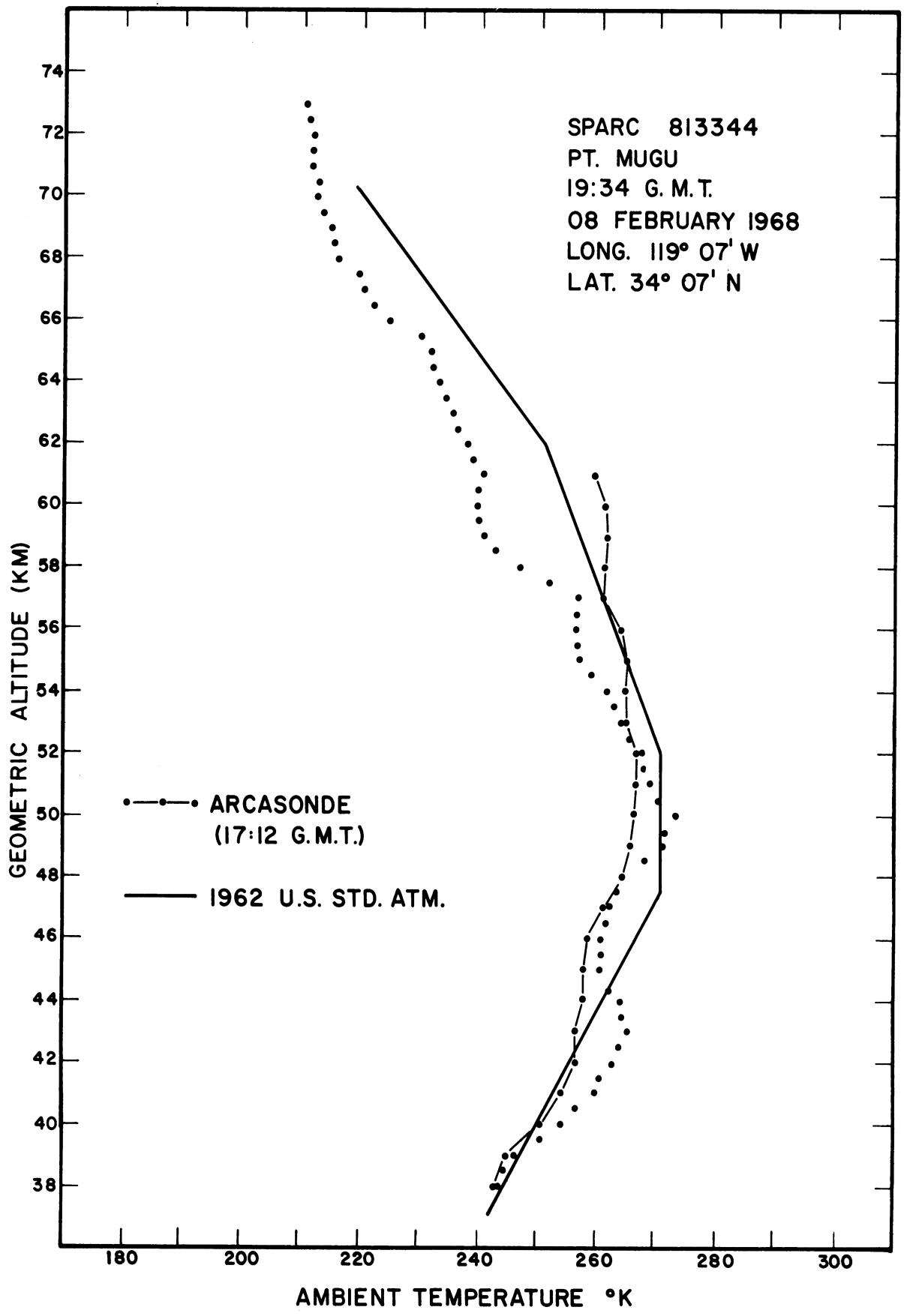

Figure 11. Altitude vs. temperature - Sparc 813344.

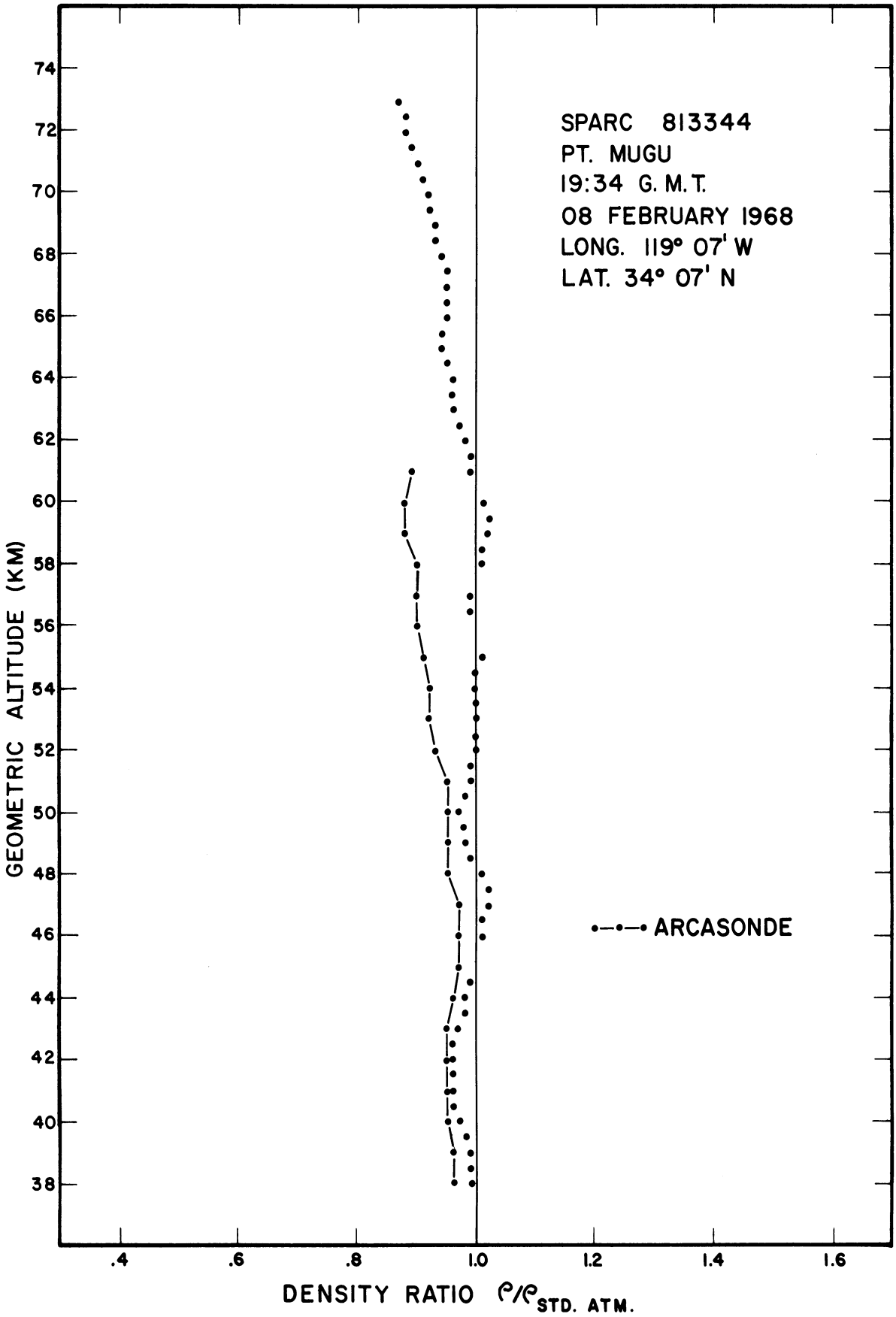

Figure 12. Altitude vs. density - Sparc 813344.

5. DISCUSSION

The Sparrow-Arcas vehicle combination proved to be a completely adequate propulsion system for researching the meososphere by the pitot technique. Simple modification of the payload geometry would permit data acquisition to approximately 105 km.

The density data obtained from the two Sparc firings were corrected for rather large errors due to horizontal wind structure, as much as 4%. This was due to the excessively low effective launch elevation angles (>80° Q.E.) and is not representative of a typical data reduction error source. An effective Q.E. of 83° would have reduced the maximum error to less than 2%. The temperature derived from the density profile is dependent on its slope, not on the absolute magnitude. The maximum temperature error resulting from an uncorrected density profile would have been less than 4°K.

6. BIBLIOGRAPHY

Ainsworth, J. E., Fox, D. F., and Lagow, H. E., "Upper Atmosphere Structure Measurement Made with the Pitot-Static Tube," Journal of Geophysical Research, 66, No. 10, 3191-3212, 1961.

Ames Research Staff, Equations, Tables, and Charts for Compressible Flow, National Advisory Committee for Aeronautics, Report No. 1135, 1953.

Atlantic Research Corporation, Final Technical Report on the Design, Fabrication and Flight Testing of a Meteorological Rocket Probe, Atlantic Research Final Report, TR-PL-6966, April 1965.

Flanick, A. P., and Ainsworth, J. E., "Vacuum Gauge Calibration System (10^{-2} to 10^{1} mmHg)," Review of Scientific Instruments, 32, No. 4, 408-410, April 1961.

Hines, P. B., Dovap Systems and Data Reduction Methods, New Mexico State University, Physical Science Laboratory, University Park, New Mexico, January 1962.

Horvath, J. J., and Rupert, G. F., Pitot Measurements on an X-15 Rocket Plane, University of Michigan Scientific Report 06093-1-F, August 1968.

Horvath, J. J., Simmons, R. W., and Brace, L. H., Theory and Implementation of the Pitot-Static Technique for Upper Atmosphere Measurements, University of Michigan Scientific Report 04673-1-S, March 1962.

Larson, T. L., and Montoya, E. J., "Stratosphere and Mesosphere Densities Measured with the X-15 Airplane," Journal of Geophysical Research, 69, No. 24, 5123-5130, December 1964.

Laurmann, J. A., Low Density Characteristics of an Aerobee-Hi Pitot-Static Probe, University of California, Institute of Engineering Research, Technical Report HE-150-156, May 1958.

El-Moslimany, M. A., Theoretical and Experimental Investigation of Radioactive Ionization Gauges, University of Michigan Scientific Report 03554-4-S, May 1960.

Murgatroyd, R. J., "Winds and Temperatures Between 20 km and 100 km—A Review," Quarterly Journal of the Royal Meteorological Society, 83, No. 358, 417-454, October 1957.

Nagy, A. F., Spencer, N. W., Niemann, H. B., and Carignan, G. R., Measurement of Atmospheric Pressure, Temperature, and Density at Very High Altitudes, University of Michigan Final Scientific Report 02804-7-F, August 1961.

Newell, H. E., High Altitude Rocket Research, Academic Press, New York, 1953.

Rupert, G. F., Engineering Design of a Pitot-Static Probe Payload, University of Michigan Engineering Report 05776-2-E, April 1967.

Schultz, F. V., Spencer, N. W., and Reifman, A., Atmospheric Pressure and Temperature Measurements Between the Altitudes of 40 and 100 Kilometers, Upper Atmosphere Report No. 2, University of Michigan Research Institute, Ann Arbor, July 1948.

Shapiro, A. H., Dynamics and Thermodynamics of Compressible Fluid Flow, 1, The Ronald Press, New York, 1953.

Sherman, F. S., New Experiments on Impact Pressure Interpretation in Supersonic and Subsonic Rarefied Airstreams, NACA Technical Note 2995, September 1953.

Simmons, R. W., An Introduction to the Theory and Data Reduction Method for the Pitot-Static Technique of Upper Atmosphere Measurement, University of Michigan Scientific Report 05776-1-S, March 1964.

U. S. Standard Atmosphere, 1962, U. S. Government Printing Office, Washington, D.C., December 1962.

CRL CONTRACTOR DISTRIBUTION LIST

AFCRL (CRMPLR) Stop 29
L. G. Hanscom Field
Bedford, Massachusetts 01730
5 Copies

AFCRL (CRMXRA) - Stop 39
L. G. Hanscom Field
Bedford, Massachusetts 01730
10 Copies

AFCRL (CRN) Stop 30
L. G. Hanscom Field
Bedford, Massachusetts 01730

AFCRL (CRTE) Stop 30
L. G. Hanscom Field
Bedford, Massachusetts 01730

AFCRL (CRTPM) Stop 30
L. G. Hanscom Field
Bedford, Massachusetts 01730

West Coast Office, AFCRL
Attn Mr. Gene M. DeGiacomo
SSTRT/CRZ
Los Angeles Air Force Station
Los Angeles, California 90045

ADC
Operations Analysis Office
Ent Air Force Base
Colorado 80912

AFAL (AVX)
Wright-Patterson AFB, Ohio 45433

AFETR
Technical Library-MU-135
Patrick AFB, Florida 32925

AFIT (MCLI-Library)
Bldg. 640 - Area B
Wright-Patterson AFB, Ohio 45433

AFSC-STLO (RSTAL)
AF Unit Post Office
Los Angeles, California 90045

AFSC-STLO (MIT)
Waltham Federal Center
424 Trapelo Road
Waltham, Massachusetts 02154

AFSC-STLO (MIT)
68 Albany St.
Cambridge, Massachusetts 02139

AFWL (WLIL)
Kirtland AFB, N.M. 87117

Director,
Air University Library
Attn AUL3T
Maxwell AFB, Alabama 36112

APGC (PGBPS-12)
Eglin AFB, Florida 32542

OAR (RRY)
1400 Wilson Blvd.
Arlington, Virginia 22209

RADC (EMTLD)
Attn Documents Library
Griffiss AFB, N.Y. 13440

RTD
Scientific Director
Bolling AFB
Washington, D. C. 20332

SAC (OA)
Offutt AFB, Nebraska 68113

FAA
Bureau of Research & Development
300 Independence Ave., S. W.
Washington, D. C. 20553

Government Printing Office
Library
Division of Public Documents
Washington, D. C. 20402

Library of Congress
Aerospace Technical Division
Washington, D. C. 20540

Library of Congress
Exchange & Gift Division
Washington, D. C. 20540

NASA Scientific & Technical
Information Facility
Attn: Acquisitions Br. (S-AK/DL)
P.O. Box 33
College, Md. 20740

NASA-Flight Research Center
Library
P.O. Box 273
Edwards, California 93523

NASA-Goddard Inst. for Space Studies
Library
2880 Broadway
New York, N.Y. 10025

NASA-Goddard Space Flight Center
Technical Library
Greenbelt, Md. 20771

NASA-Jet Propulsion Laboratory
Attn: Library (TDS)
4800 Oak Grove Dr.
Pasadena, California 91103

NASA-Lewis Research Center
Library - Mail Stop 60-3
21000 Brookpark Road
Cleveland, Ohio 44135

NASA-Manned Spacecraft Center
Technical Library (Code BM63)
Houston, Texas 77058

National Center for Atmospheric
Research
NCAR Library, Acquisitions
Boulder, Colorado 80302

ODDR & E (Library)
Room 3C-128
The Pentagon
Washington, D. C. 20301

Aerospace Corporation
Attn: Library Acquisitions Group
P.O. Box 95085
Los Angeles, California 90045

Battelle Memorial Institute
Library
505 King Avenue
Columbus, Ohio 43201

The Mitre Corp.
Attn: Library
P.O. Box 208
Bedford, Massachusetts 01730

The Rand Corporation
Attn: Library-D
1700 Main St.
Santa Monica, California 90406

SAMSO (SMTTA)
AF Unit Post Office
Los Angeles, California 90045

Hq TAC (OA)
Langley AFB, Virginia 23362

USAF Academy
Academy Library (DFSLB)
Colorado 80840

Army Missile Command
Attn: Chief, Document Section
Redstone Scientific Info. Ctr.
Redstone Arsenal, Alabama 35809

U. S. Army Electronics Command
Attn: AMSEL-RD-MAT
Technical Document Center
Fort Monmouth, N. J. 07703

U. S. Army Research Office
Attn: Technical Library
3050 Columbia Pike
Arlington, Virginia 22204

Naval Ordnance Laboratory
Technical Library
White Oak
Silver Spring, Md. 20910

Commanding Officer
Office of Naval Research Branch Off.
Box 39 - Fleet Post Office
New York, N.Y. 09510
2 Copies

Director
Naval Research Laboratory
Attn: 2027
Washington, D. C. 20390

U. S. Naval Ordnance Test Station
Attn Technical Library
China Lake, California 93555

U. S. Naval Postgraduate School
Library (Code 2124)
Monterey, California 93940

U. S. Navy Electronics Laboratory
(Library)
San Diego, California 92152

Central Intelligency Agency
Attn: OCR/DD/STD Distribution
Washington, D. C. 20505

Clearinghouse for Federal Scientific
& Technical Information (CFSTI)
Sills Building
5285 Port Royal Rd.
Springfield, Virginia 22151

Director
Defense Atomic Support Agency
Washington, D. C. 20305
2 Copies

DIA
(DIAAP-142)
Washington, D. C. 20301

Environmental Sciences Services Adm
Library
Boulder Laboratories
Boulder, Colorado 80302
2 Copies

British Defence Staffs
British Embassy
Scientific Information Officer
3100 Mass. Ave., N. W.
Washington, D. C. 20008
3 Copies

Chief, Canadian Defence Research Staff
2450 Mass. Ave., N. W.
Washington, D. C. 20008
3 Copies

National Research Council
National Science Library
Ottawa 7, Canada

AWVAS
Attn: Robert G. Stone
Scientific & Technical Information
Office
Hq Air Weather Service
Scott AFB, Illinois 62225

Defense Documentation Center (DDC)
Cameron Station
Alexandria, Virginia 22314
20 Copies

AFCRL (CRMXRP) Stop 30
L. G. Hanscom Field
Bedford, Massachusetts 01730

AIAA-TIS Library
750 Third Avenue
New York, N. Y. 10017

AFCRL (CRES) Stop 30
Attn: Gerard H. Faucher
L. G. Hanscom Field
Bedford, Massachusetts 01730
10 Copies

Unclassified

Security Classification

DOCUMENT CONTROL DATA - R & D

(Security classification of title, body of abstract and indexing annotation must be entered when the overall report is classified)

1. ORIGINATING ACTIVITY (Corporate author)	2a. REPORT SECURITY CLASSIFICATION
The University of Michigan Space Physics Research Lab., Dept. of Electrical Engr. Ann Arbor, Michigan 48105	Unclassified 2b. GROUP

3. REPORT TITLE

PITOT MEASUREMENTS ON SPARROW-ARCAS VEHICLES

4. DESCRIPTIVE NOTES (Type of report and inclusive dates)

Scientific Final. 1 April 1965 through 31 August 1968. Approved 6 June 1969

5. AUTHOR(S) (First name, middle initial, last name)

Jack J. Horvath

6. REPORT DATE	7a. TOTAL NO. OF PAGES	7b. NO. OF REFS
June 1969	30	19

8a. CONTRACT OR GRANT NO.	9a. ORIGINATOR'S REPORT NUMBER(S)
AF19(628)-5069 b. PROJECT, Task, Work Unit Nos. 6682-02-01 c. DoD Element 65701F d. DoD Subelement 676682	07301-1-F 9b. OTHER REPORT NO(S) (Any other numbers that may be assigned this report) AFCRL-69-0241

10. DISTRIBUTION STATEMENT

Distribution of this document is unlimited. It may be released to the Clearinghouse, Department of Commerce, for sale to the general public.

11. SUPPLEMENTARY NOTES	12. SPONSORING MILITARY ACTIVITY
TECH, OTHER	Air Force Cambridge Research Laboratories (CRE) L. G. Hanscom Field Bedford, Massachusetts 01730

13. ABSTRACT

Radioactive ionization gages were used as sensors for pitot measurements on two Sparrow-Arcas boosted payloads launched on 7 and 8 February 1968. Pressure, temperature, and density were obtained in the region 38 to 70 km. Both graphical and tabulated data are presented.

The vehicle system performance and the payload performance were excellent. Modification of ionization gage sensitivity would permit data acquisition to 105 km.

DD FORM 1 NOV 68 1473

Unclassified

Security Classification

14. KEY WORDS	LINK A		LINK B		LINK C	
	ROLE	WT	ROLE	WT	ROLE	WT
Pitot Sensing System						
Atmospheric Structure Measurement						
Radioactive Ionization Gages						